

SCIENTIFIC REPORTS



OPEN

The N-terminal sequence of the extrinsic PsbP protein modulates the redox potential of Cyt b_{559} in photosystem II

Taishi Nishimura¹, Ryo Nagao², Takumi Noguchi², Jon Nield³, Fumihiko Sato¹ & Kentaro Ifuku¹

Received: 27 October 2015

Accepted: 25 January 2016

Published: 18 February 2016

The PsbP protein, an extrinsic subunit of photosystem II (PSII) in green plants, is known to induce a conformational change around the catalytic Mn_4CaO_5 cluster securing the binding of Ca^{2+} and Cl^- in PSII. PsbP has multiple interactions with the membrane subunits of PSII, but how these affect the structure and function of PSII requires clarification. Here, we focus on the interactions between the N-terminal residues of PsbP and the α subunit of Cytochrome (Cyt) b_{559} (PsbE). A key observation was that a peptide fragment formed of the first N-terminal 15 residues of PsbP, 'pN15', was able to convert Cyt b_{559} into its HP form. Interestingly, addition of pN15 to NaCl-washed PSII membranes decreased PSII's oxygen-evolving activity, even in the presence of saturating Ca^{2+} and Cl^- ions. In fact, pN15 reversibly inhibited the S_1 to S_2 transition of the OEC in PSII. These data suggest that pN15 can modulate the redox property of Cyt b_{559} involved in the side-electron pathway in PSII. This potential change of Cyt b_{559} , in the absence of the C-terminal domain of PsbP, however, would interfere with any electron donation from the Mn_4CaO_5 cluster, leading to the possibility that multiple interactions of PsbP, binding to PSII, have distinct roles in regulating electron transfer within PSII.

The oxygen-evolving reactions are a fundamental component of Life and critical to the evolutionary success underpinning the conversion of sunlight to chemical energy. This chemistry is performed within a protein-ligand-cofactor micro-environment termed the Oxygen-Evolving Complex (OEC), extending out from the luminal surface of membrane-bound photosystem II (PSII)¹. Much progress has been made toward determining the structure of the PSII complex and recent X-ray structural analysis of the prokaryotic, cyanobacterial, PSII complex at atomic resolution has revealed the location of >20 membrane-intrinsic and -extrinsic protein subunits, pigments, and redox cofactors, including a metal cluster of four Mn ions, Ca^{2+} , and five oxo ligands, together termed the Mn_4CaO_5 cluster^{2,3}.

Light excitation of the primary donor P680, a special pair of chlorophyll (Chl) *a* dimers in PSII, leads to primary charge separation and subsequent electron transfer to a nearby pheophytin, which is followed by further electron transfer via two quinones, Q_A and Q_B . The oxidative hole remaining on P680 is transferred to the Mn_4CaO_5 cluster via a redox-active tyrosine, Tyr¹⁶¹, on the D1 subunit. The Mn_4CaO_5 cluster converts two water molecules into one molecule of oxygen and four protons through a light driven cycle consisting of five intermediates called S_i states ($i = 0-4$)⁴. Among them, the S_1 state is the most dark-stable, and flash illumination advances each S_i state ($i = 0-3$) to the next S_{i+1} state. Molecular oxygen is released during the $S_3-S_4-S_0$ transition after the transient S_4 state⁵.

In addition, PSII has a side-electron pathway mediated by at least the Cyt b_{559} , formed of the PsbE and PsbF subunits, carotenoids, and a chlorophyll, Chl_z, that together function as a safety valve to remove the excess oxidative hole from the donor side, although the detail of this side-electron pathway is still a subject of much debate⁶. Cyt b_{559} is known to have several forms that differ in their redox potential: the high-potential (HP) form, the intermediate-potential (IP) form and the low-potential (LP) form⁷. It has been hypothesized that Cyt b_{559} may

¹Graduate School of Biostudies, Kyoto University, Sakyo-ku, Kyoto 606-8502, Japan. ²Graduate School of Science, Nagoya University, Aichi 464-8602, Japan. ³School of Biological and Chemical Sciences, Queen Mary University of London, London E1 4NS, United Kingdom. Correspondence and requests for materials should be addressed to K.I. (email: ifuku@kais.kyoto-u.ac.jp)

interconvert amongst its various redox states dependent upon any ongoing donor- and acceptor-side inhibition of PSII, and thus contributes to the protection of PSII from photodamage⁸.

The composition of membrane-intrinsic PSII core subunits is highly conserved among photo-oxygenic organisms, while the make-up of the extrinsic protein domain has undergone significant change during evolution⁹. Green plants, including higher plants, have a set of three extrinsic proteins, PsbO, PsbP, and PsbQ¹⁰. In contrast, cyanobacteria have PsbO in common, but feature PsbV (Cyt *c*₅₅₀) and PsbU instead of PsbP and PsbQ¹¹. It has also been reported that cyanobacteria possess PsbP and PsbQ homologs, termed CyanoP and CyanoQ¹². The current view is that PsbV and PsbU have been lost during evolution, and PsbP and PsbQ in green plants appear to have evolved from CyanoP and CyanoQ, respectively¹³. Furthermore, higher plants have multiple homologs of PsbP and PsbQ. In Arabidopsis, two PsbP proteins (PsbP1 and PsbP2), two PsbQ proteins (PsbQ1 and PsbQ2), two PsbP-like proteins (PPL1 and PPL2), seven PsbP-domain proteins (PPD1-7), and three PsbQ-like proteins (PQL1-3) have been identified¹⁴. Genetic studies using Arabidopsis mutants have demonstrated that PsbP and PsbQ homologs are actually involved not only in PSII regulation and PSII repair, but also in chloroplast NDH activity and PSI assembly^{15,16}. However, the exact reason as to why green plants have developed PsbP and PsbQ, specifically, for binding to PSII, remains to be answered¹⁷.

The molecular function of the PsbP and PsbQ proteins has been studied both *in vitro* and *in vivo*. For the former, *in vitro* release-reconstitution experiments using isolated oxygen-evolving PSII membranes have shown PsbP and PsbQ to be responsible for the retention of Ca²⁺ and Cl⁻ within the OEC, essential cofactors for the oxygen-evolving, or water-splitting, reactions^{18,19}. Fourier transform infrared (FTIR) difference spectroscopy has elucidated that PsbP, but not PsbQ, induces protein conformational changes around the Mn₄CaO₅ cluster to modulate the binding properties of Ca²⁺ and Cl⁻²⁰. Analysis of knockout and knockdown plants has revealed that PsbP is essential for plant photo-autotrophy and assembly of PSII²¹⁻²⁴, while PsbQ is only required for PSII stability under low light conditions²⁵. Therefore, the interaction between PsbP and PSII is particularly important for optimising and enhancing oxygen-evolution, while PsbQ has an auxiliary function to stabilize the functional interaction of PsbP with PSII²⁶.

Recent chemical cross-linking experiments using 1-ethyl-3-(3-dimethylaminopropyl) carbodiimide (EDC) suggest that PsbP has multiple interactions in a higher plant PSII supercomplex; PsbP directly interacts with the Cyt *b*₅₅₉ α subunit (the PsbE protein) via its N-terminus, and also with PsbR²⁷. In addition, PsbP interacts with both CP26 and CP43 light-harvesting proteins via the amino-acid residues located in its C-terminal domain²⁸. We previously reported that PsbP- Δ 15, in which the highly conserved N-terminus 15-residues are truncated, loses the ability to induce protein conformational change around the Mn₄CaO₅ cluster, and did not induce any oxygen-evolution^{20,29}. This N-terminal sequence of PsbP is invisible in the current structural models and should take an extending flexible structure^{30,31}. The binding of PsbQ, however, can restore the function of PsbP- Δ 15²⁶, indicating that the N-terminal sequence of PsbP is not essential for the retention of ions in the OEC and may have other functions.

In this study, we investigated the importance of the interaction of PsbP with PSII via its N-terminus. Reduced-minus-oxidized spectra of Cyt *b*₅₅₉ showed that the redox potential change of Cyt *b*₅₅₉ occurs through association of native PsbP protein, but not by N-terminal truncated PsbP. Intriguingly, a synthetic pN15 peptide, which consists of PsbP N-terminal 15 residues, affects the structure of Cyt *b*₅₅₉ in a transmembrane manner and triggers the redox potential change of the haem in Cyt *b*₅₅₉. Furthermore, the pN15 peptide reduces the oxygen-evolving activity of PSII and inhibits the S₁ to S₂ transition in the OEC suggested by thermoluminescence (TL) and FTIR. The above observations indicate for the first time that a novel mechanism exists for modulating the redox property of Cyt *b*₅₅₉ which may simultaneously affect the internal electron transfer within PSII by a lumenally bound extrinsic subunit, PsbP.

Results

N-terminal sequence of PsbP modulates the redox potential of Cyt *b*₅₅₉ in PSII. Figure 1 depicts the presumptive binding model of the latest X-ray structure of spinach PsbP protein (PDB ID 4RT1)³¹ fitted into the cyanobacterial PSII structure (PDB ID 3ARC)² based upon chemical cross-linking experiments^{27,28}. Only the membrane protein subunits that would interact directly with PsbP are shown. PsbP is proposed to bind to CP43 whilst extending its N-terminal sequence to interact with PsbE on the thylakoid luminal side²⁸. Although the N-terminal 11 residues of PsbP are disordered, being absent from the crystal structure, they have sufficient length to reach any site cross-linked by EDC (Ala¹ in PsbP and Glu⁵⁷ in PsbE). Another model for PsbP localization has also been proposed, where the N-terminal sequence of PsbP takes on a more compact structure, but still maintains the possibility of interacting with PsbE³². Due to these differences, we decided to investigate more thoroughly the effect of such interactions, between the PsbP N-terminus and the PsbE subunit of Cyt *b*₅₅₉, on the overall structure and function of PSII.

Firstly the effect of the association of native PsbP and PsbP- Δ 9 was investigated, the latter a mutated PsbP protein which lacks the last 9 residues of the N-terminus but retains the ability to activate the oxygen-evolving abilities of PSII^{10,33}. Spinach PSII membranes were treated with 1.5 M NaCl to remove native PsbP and PsbQ proteins, and then the PsbP protein was reconstituted back to the NaCl-washed PSII membranes at a molar ratio of 4:1 (PsbP:PSII) (Fig. S1). All redox forms of Cyt *b*₅₅₉ were first oxidized by ferricyanide, followed by its stepwise reduction with hydroquinone, ascorbate, and dithionite, all of which can be monitored by absorption difference spectroscopy³⁴. An averaged reduced-minus-oxidized spectrum for each PSII sample is shown in Fig. 2A, and the ratios of various redox forms of Cyt *b*₅₅₉ are presented in Fig. 2B. Intact PSII membranes were observed to contain about 59% of the HP form, 32% of the IP form, and 9% of the LP form. In NaCl-washed PSII membranes, the HP content was reduced to about 34% and instead the IP and LP contents were increased. In this way the dissociation of PsbP and PsbQ induced the conversion of Cyt *b*₅₅₉ into its lower redox potential form, while reconstitution of PsbP restored the HP content to about 58%, as reported previously^{35,36}. However, reconstitution of PsbP- Δ 9 was

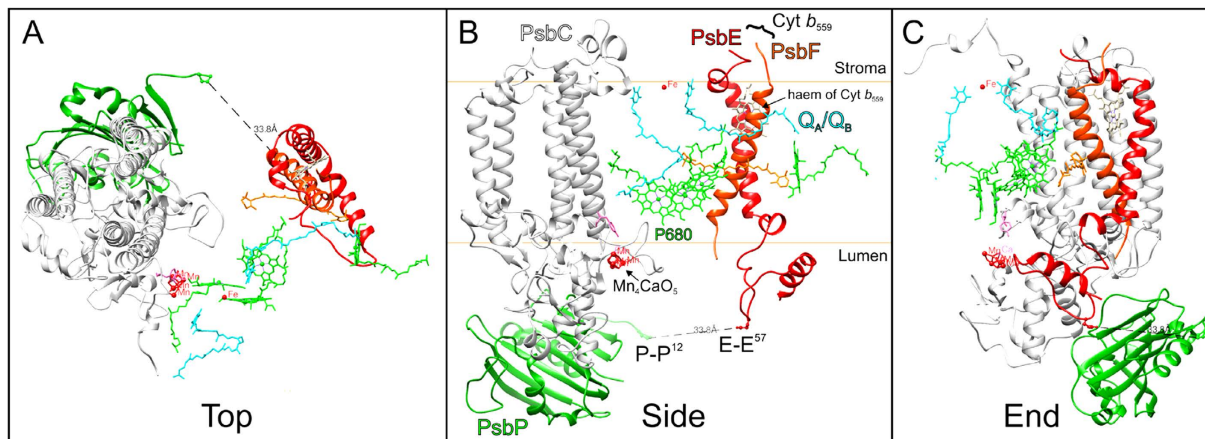


Figure 1. A presumptive model showing the binding of PsbP to the PSII complex. Set within an approximate membrane domain certain intrinsic and extrinsic subunits, CP43 (grey), Cyt b_{559} (red), and PsbP (green) are shown in cartoon ribbon form. The particular cofactor molecules, P680 (green), ChlZ (green), Q_A/Q_B (blue), haem (beige), β -carotene (orange) are rendered in stick model form. The Mn_4CaO_5 cluster and TyrZ of the D1 subunit (D1-Tyr¹⁶¹; in pink) are also presented, but visualised as surface rendered spheres and stick models, respectively. The Pro¹² in PsbP and Glu⁵⁷ in PsbE, are shown as stick models, accompanied by estimated distances. UCSF Chimera⁶² was used as the software modelling environment.

less efficient in restoring the HP content, indicating that the N-terminal sequence of PsbP was playing a significant role in the plant's ability to restore HP Cyt b_{559} into PSII.

Surprisingly, reconstitution of pN15 alone, a peptide fragment consisting of the first N-terminal 15 residues of PsbP (NH₂-AYGEAANVFGKPKKN-CONH₂), at the molar ratio of 200:1 (pN15:PSII), was able to restore the amount of the HP form to ~52% without activating the OEC (Fig. S2). This effect was not observed with the peptide when it was lacking its N-terminal Ala¹ (pN15- ΔA^1). The above results suggest that the interaction of the N-terminal sequence of PsbP with PsbE, on the luminal side of the thylakoid, affects the redox properties of the haem of Cyt b_{559} in a manner that traverses the membrane and one that is independent from the oxygen-evolving activity of PSII.

The pN15 fragment interacts with PsbE and alters the conformation of Cyt b_{559} . To confirm that pN15 interacts with PsbE in PSII, pN15 was cross-linked to PSII using EDC, a chemical cross-linker. EDC, a zero length cross-linker, cross-links a primary amine and a carboxyl group when electrostatically associated. Subsequently, the cross-linked PSII complexes were analysed by SDS-PAGE and any cross-linked products were visualized by immunoblotting using specific antibodies. The results of the immunoblotting, for PSII membranes cross-linked in the presence or absence of pN15 reconstitution, are shown in Fig. 3. No specific band appeared in the PsbO and D1 immunoblots, indicating that pN15 did not affect those particular subunits (Fig. 3C,D). A specific band did appear in the PsbE immunoblot in the presence of pN15 at approximately 11 kDa (Fig. 3A). This band was not observed when PSII was treated with EDC in the absence of pN15 and its intensity was dependent upon the amount of pN15 used during reconstitution. The molecular mass of this cross-linked product was consistent with the theoretical molecular mass of the pN15-PsbE cross-linked product (MW: 10.8 kDa).

Notably, the intensity of the band at approximately 13 kDa was seen to be inversely correlated with the amount of pN15 used for reconstitution (Fig. S3), indicating that cross-linking between PsbE and the small subunit of ~4 kDa would be concomitantly inhibited by pN15. It was inferred that this cross-linking partner of 4 kDa is most likely to be the PsbF protein, the partner of PsbE; together PsbE and PsbF form the complete Cyt b_{559} entity^{6,37}. Hence immunoblotting analysis was performed using antibodies raised against PsbF (Fig. 3B). Indeed, a band at approximately 4 kDa was identified as that of PsbF. Of interest, this band disappeared when PSII was treated with EDC in the presence of pN15. This suggested that when pN15 is reconstituted with PSII, PsbF underwent modifications by EDC to such an extent it was no longer recognized by peptide antibodies raised against PsbF. Consistent with this, the cross-linked product, expected to be approximately 13 kDa, was also not detected in the immunoblots. The PsbF antibody used recognised the N-terminal regions of PsbF, those that bind the redox haem on the stromal side (Figs S4 and S5). Therefore, pN15 would affect the structure around the redox haem of Cyt b_{559} in a manner that traverses the membrane.

pN15 peptide decreases the oxygen-evolving activity of salt-washed PSII membranes. To further investigate how the PsbP N-terminus affects the structure and function of PSII, the pN15 peptide fragment was introduced using reconstitution studies and its effect on the water-splitting reaction analysed. The oxygen-evolving capability of reconstituted PSII membranes was measured in the presence of 5 mM CaCl₂, where reconstitution of PsbP has been shown to be unnecessary for oxygen evolution^{38,39} (Fig. S6). Interestingly, the rate of oxygen-evolution for PSII membranes was decreased by reconstitution of pN15 even in the presence of 5 mM CaCl₂, and the reduction in rate of oxygen-evolution was dependent on the amount of pN15 reconstituted

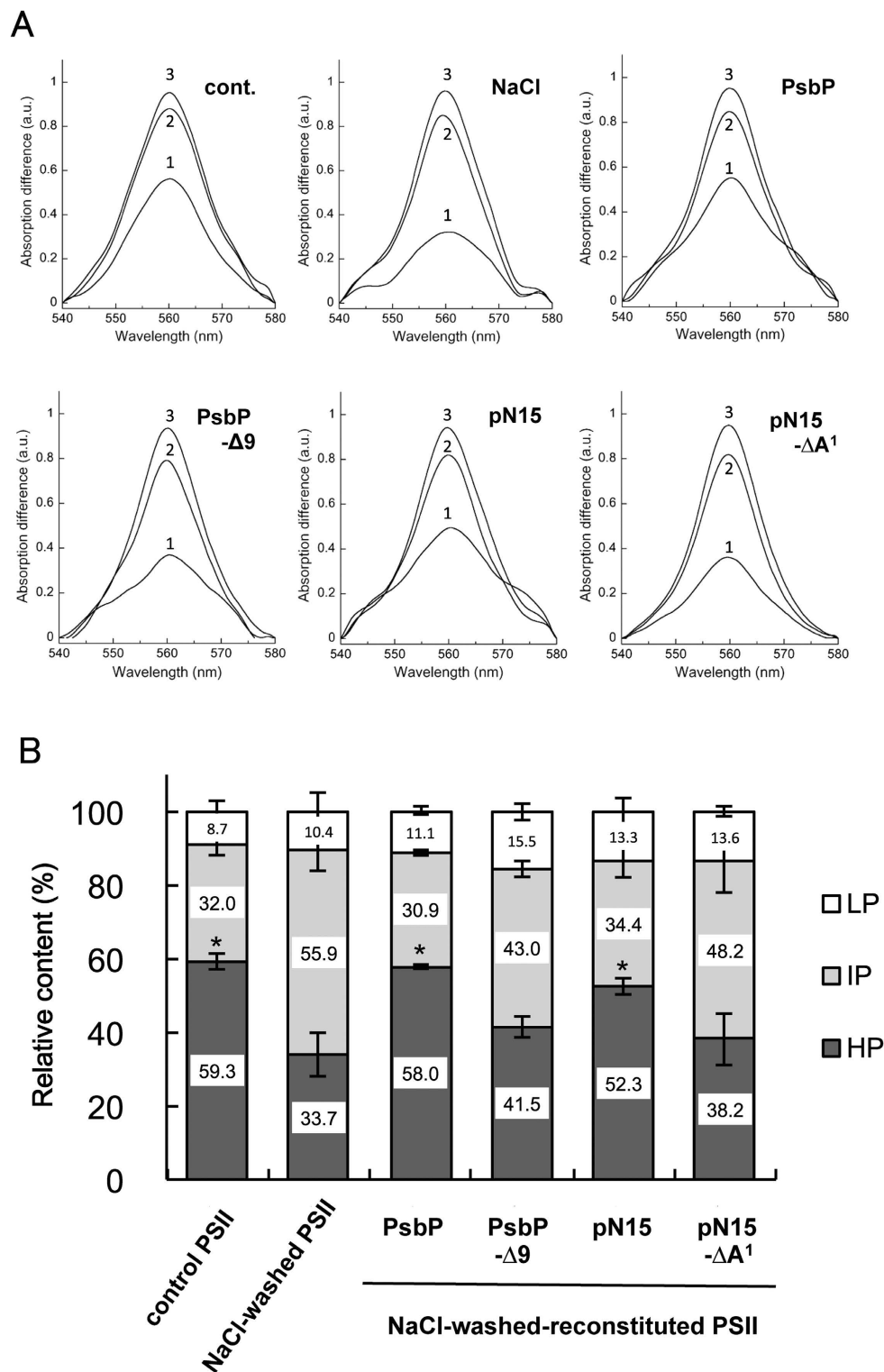


Figure 2. Changes in the redox potential of Cyt b_{559} when induced by PsbP. (A) Reduced minus oxidized spectra of Cyt b_{559} in untreated (cont.), NaCl-treated (NaCl), PsbP-reconstituted (PsbP), PsbP- $\Delta 9$ -reconstituted (PsbP- $\Delta 9$), pN15-reconstituted (pN15), and pN15- ΔA^1 -reconstituted (pN15- ΔA^1) PSII membranes. Hydroquinone-reduced minus ferricyanide-oxidized (1), ascorbate-reduced minus ferricyanide-oxidized (2), and dithionite-reduced minus ferricyanide-oxidized (3) difference spectra were used to estimate the amount of the HP, IP, and LP forms of Cyt b_{559} , respectively. Each spectrum was an average of three independent measurements and normalized to the peak of the dithionite-reduced minus ferricyanide-oxidized difference spectrum. (B) Relative content of the HP, IP, and LP forms of Cyt b_{559} determined by stepwise reductive titration. Total amount of Cyt b_{559} is set as 100%. The asterisks indicate the significant increase of the content of the HP Cyt b_{559} by reconstitution. (* $p < 0.05$, Student's t -test; $n = 3$, error bars = SEM).

(Fig. 4A). This demonstrates that pN15 has an inhibitory effect on the rate of oxygen evolution. Simultaneous reconstitution of pN15 and full-length (intact) PspB did not inhibit the oxygen-evolving reaction (Fig. S6). This suggests that intact PspB can eliminate the inhibitory effect of pN15. Therefore, the inhibitory effect of pN15 was not due to non-specific interaction with PSII.

The effects of pN15- ΔA^1 and other mutated pN15 peptide fragments, in which the N-terminal Ala¹ was substituted with other residues (Gly, Asp, Lys, or Trp), or an additional Trp residue was added to the N-terminus (depicted as A¹G, A¹D, A¹K, A¹W, and W-A¹, respectively), were also investigated. In contrast to the native pN15 fragment, none of these mutated pN15 fragments showed any inhibitory effect on oxygen evolution, indicating that the N-terminal Ala¹ is crucial for the inhibitory effect of pN15. Furthermore, a pN27 peptide fragment, consisting of the first 27 residues of the N-terminus, was prepared and its reconstitution was observed to decrease the rate of oxygen-evolution by the PSII membranes in a manner similar to pN15. This showed that an extension of peptide length, from 15 up to 27 residues, does not significantly change the inhibitory effect of pN15 on water-splitting. The estimated dissociation constant (K_d value) of pN15 to PSII complex was $\sim 5.9 \times 10^{-7}$ M. Such a high K_d value certainly suggests that the binding affinity of pN15 to the PSII core complex is relatively low.

Cross-linking experiments using mutated pN15 and pN27 peptide fragments were also performed (Fig. S7). When mutated pN15 peptides were used, the cross-linked band of ~ 11 kDa was greatly decreased, suggesting that the N-terminal residue of pN15 is indeed important for the interaction with PspE. Furthermore, when pN27 peptide fragments were used for cross-linking experiments, the new band appeared at ~ 13 kDa in the stead of the band ~ 11 kDa. In summary, pN15 interacts with PspE in the same way as intact PspB and affects the conformation and interaction between the Cyt b_{559} subunits, PspE and PspF.

We next examined if the inhibitory effect of pN15 on PSII was reversible or not. The PSII sample reconstituted by pN15 was washed once with the buffer used for reconstitution, and then the oxygen-evolving activity was measured in the presence of 5 mM CaCl₂ and 5 mM NaCl (Fig. 4B). The rate of oxygen-evolution of PSII, washed after pN15 reconstitution, was restored to almost the same level of the control PSII sample, indicating that the inhibitory effect of pN15 is reversible. It also suggests that the imperfect inhibition of oxygen-evolving activity by pN15 might also be caused by its partial dissociation away from PSII upon dilution with the assay buffer.

pN15 inhibits the S₁ to S₂ transition of the OEC. To examine further the inhibitory effect of pN15 on light-induced charge separation within PSII, thermoluminescence (TL) measurements were conducted on NaCl-washed PSII samples (the control PSII) and pN15-reconstituted PSII membranes (reconstitution was performed at a molar ratio of 200:1) in the presence of 5 mM CaCl₂ and 5 mM NaCl (Fig. 5A). TL originates from a PSII reaction centre that is re-excited by a charge recombination due to an increase in the temperature within the samples, where light-induced charge pairs in PSII had been freeze-trapped⁴⁰. The B-band arises from a recombination of the S₂/S₃ state, of the Mn₄CaO₅ cluster, with Q_B⁻⁴¹. In the control PSII, B-bands were observed around 37 °C, however, B-band intensity in pN15-reconstituted PSII was significantly decreased. Of note, the opposite occurred with pN15- ΔA^1 moderately decreasing the intensity of the B-band. Afterwards, the intensity of the B-band for pN15-reconstituted PSII was restored to that of control PSII sample levels by washing with buffer, suggesting that pN15 reversibly inhibits the S₂/S₃Q_B⁻ charge separation within PSII (Fig. S8).

The inhibitory effect of pN15 on the oxygen-evolving mechanism was further examined by FTIR analysis. FTIR difference spectroscopy is able to detect subtle structural changes coupled to oxygen-evolution, including the conformational changes in polypeptide subunit main chains, amino acid side chains, the core structure of the Mn₄CaO₅ cluster, and substrate and functional water molecules⁴². The S₂/S₁ FTIR difference spectra of NaCl-washed, and pN15-reconstituted PSII membranes, are shown in Fig. 5B. Prominent bands at 1700–1600 and 1450–1300 cm⁻¹ mainly arise from the amide I vibrations (C=O stretches of backbone amides) of polypeptide main chains and the symmetric COO⁻ stretching vibrations of surrounding carboxylate groups, respectively, while bands at 1600–1500 cm⁻¹ arise from either the amide II vibrations (NH bends coupled with the CN stretches of backbone amides) or the asymmetric COO⁻ vibrations. It was previously shown that features in the amide I region were perturbed by washing with NaCl but recovered by PspB binding²⁰. However, rebinding of pN15 to NaCl-washed PSII membranes did not recover the amide I bands; on the contrary, it diminished the entire spectral changes in the 1800–1200 cm⁻¹ region and the spectral intensity was mostly lost when reconstitution was performed with a molar ratio of 200:1 (pN15:PSII). In contrast, addition of the pN15- ΔA^1 with a ratio of 200:1 showed a moderate inhibitory effect. These data once more indicate that the S₁ to S₂ transition was severely inhibited by pN15. To be noted is that differences in the extent of inhibition among the different analyses might be caused by a low binding affinity of pN15 with PSII: Reconstituted PSII membranes were used without dilution in TL analysis, and they were further concentrated as a hydrated film used in FTIR, while samples are necessarily diluted in the measurements of oxygen-evolving activity. Overall, it is concluded that pN15 reversibly inhibits the S₁ to S₂ transition of the OEC in PSII.

Discussion

It is recognized that PspB induces conformational change around the OEC to allow for Ca²⁺ and Cl⁻ ions to bind with high affinity²⁰. In our study, a distinct regulatory mechanism via the N-terminal domain of PspB has been elucidated, given that the reconstitution of PspB, as well as pN15, affects the redox potential of Cyt b_{559} ; both convert the Cyt b_{559} in NaCl-washed PSII membranes into the HP form, albeit imperfectly. In fact, pN15 interacts with PspE and affects the structural conformation of Cyt b_{559} directly. Interestingly, for the oxygen-evolving activity, FTIR, and TL measurements suggest that pN15 reversibly inhibits the S₁ to S₂ transition of the OEC. Currently, a direct relationship between the two observations above has not been demonstrated. One possibility is that some of the oxidative hole around P680 were transferred to the HP form of Cyt b_{559} , causing a reduction in oxygen-evolution during the presence of pN15. For intact PspB, its N-terminal sequence did not prevent oxygen-evolution because the secondary electron transfer pathway, via Cyt b_{559} , is unable to compete with the

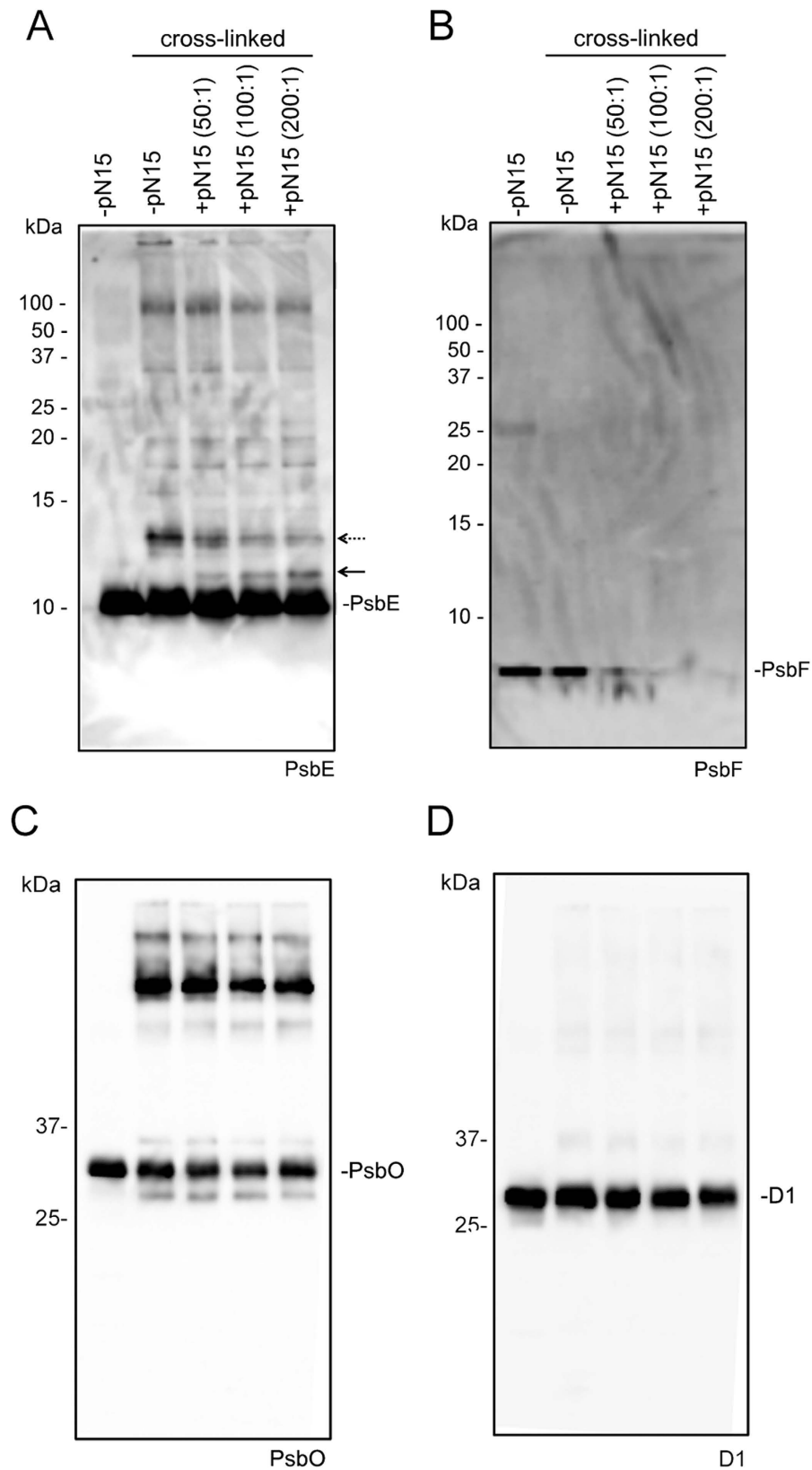


Figure 3. Cross-linking of the pN15 fragment with PSII membranes using EDC and sulfo-NHS. NaCl-washed PSII membranes were cross-linked with pN15 at a molar pN15:PSII ratio of 50:1 to 200:1. For each sample, an amount of protein corresponding to 3 μ g Chl was loaded onto each lane and detected with antisera against PsbE (A), PsbF (B), PsbO (C), and D1 (D). The arrow at ~11 kDa indicates the peptide of pN15 cross-linked to PsbE. The dashed arrow at ~13 kDa indicates the putative peptide of PsbE cross-linked to PsbF. The original positions of PsbE (9 kDa), PsbF (4 kDa), PsbO (33 kDa), and D1 (32 kDa) subunits are also indicated.

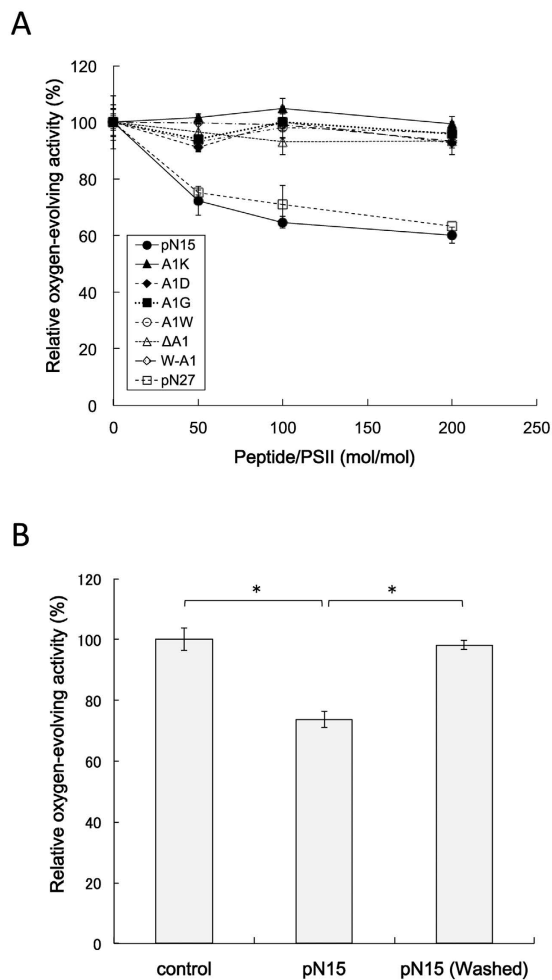


Figure 4. Oxygen-evolving activity of PSII membranes reconstituted with pN15, the N-terminal peptide of PsbP. (A) Reconstitution of various pN15 fragments was performed at a molar pN15:PSII ratio of 50:1 to 200:1. PSII oxygen-evolving activity was measured in the presence of 5 mM CaCl_2 and 5 mM NaCl, and the rate of oxygen-evolution of PSII membranes without reconstitution was set at 100% ($251 \sim 317 \mu\text{mol O}_2 \text{ mg Chl}^{-1} \text{ h}^{-1}$ in independent experiments); $n = 3$, error bars = SEM. (B) Oxygen-evolving activity of pN15-reconstituted PSII membranes with or without a washing step. Reconstitution was performed at a molar pN15:PSII ratio of 200:1. Oxygen-evolving activity here was measured in the presence of 5 mM CaCl_2 and 5 mM NaCl, and the rate of oxygen-evolution for the PSII membranes without reconstitution (the control) was set at 100% ($261 \mu\text{mol O}_2 \text{ mg Chl}^{-1} \text{ h}^{-1}$). The asterisks indicate the significant difference ($*p < 0.01$, Student's *t*-test); $n = 3$, error bars = SEM.

electron donation from the Mn_4CaO_5 cluster in intact PSII⁶. We thus propose that PsbP has a dual function to activate primary electron transfer from the Mn_4CaO_5 cluster and also to secure secondary electron transfer to P680^{*+} . This would allow a fine balance between the donor and acceptor reactions within PSII to be effected. Our results may also be relevant to previous observations showing that any removal of PsbP and PsbQ affect the electron transfer on the reducing side of PSII^{43,44}.

Structural differences among different redox forms of Cyt b_{559} are unknown. A conversion from the HP to LP, or IP, forms of Cyt b_{559} has been observed under various conditions including salt- and Tris-washing of PSII membranes, while the conversion into HP Cyt b_{559} has proven to be more difficult to achieve experimentally⁶. It has been proposed that differences in redox potential are due to the protein environment around the haem⁷. We were unable to identify any cross-linking sites between PsbE and PsbF, however, a possible crosslinking site might be found on the stromal side, where the PsbF antibody also recognized its epitope (Fig. S4). In the cyanobacterial PSII structure, Glu⁶ of PsbE and Arg¹⁸ of PsbF, both highly conserved from cyanobacteria to higher plants, are closely located near the haem and its axial His ligands (Fig. S5). Indeed, mutations of the residues on the cytoplasmic side of Cyt b_{559} are reported to affect the redox properties of Cyt b_{559} ⁴⁵. Therefore, it is likely that the interaction of pN15 with PsbE on the luminal side would change the interaction between PsbE and PsbF in their stromal-facing regions, thus transforming the redox properties of Cyt b_{559} .

It has been proposed that PsbP has a “catalytic” function, in addition to its structural role as an OEC subunit protecting the Mn_4CaO_5 cluster during the assembly of PSII^{15,16}. In fact, complete elimination of PsbP in an *Arabidopsis* mutant impairs the photo-autotrophy that causes a seedling-lethal phenotype, while a minimum

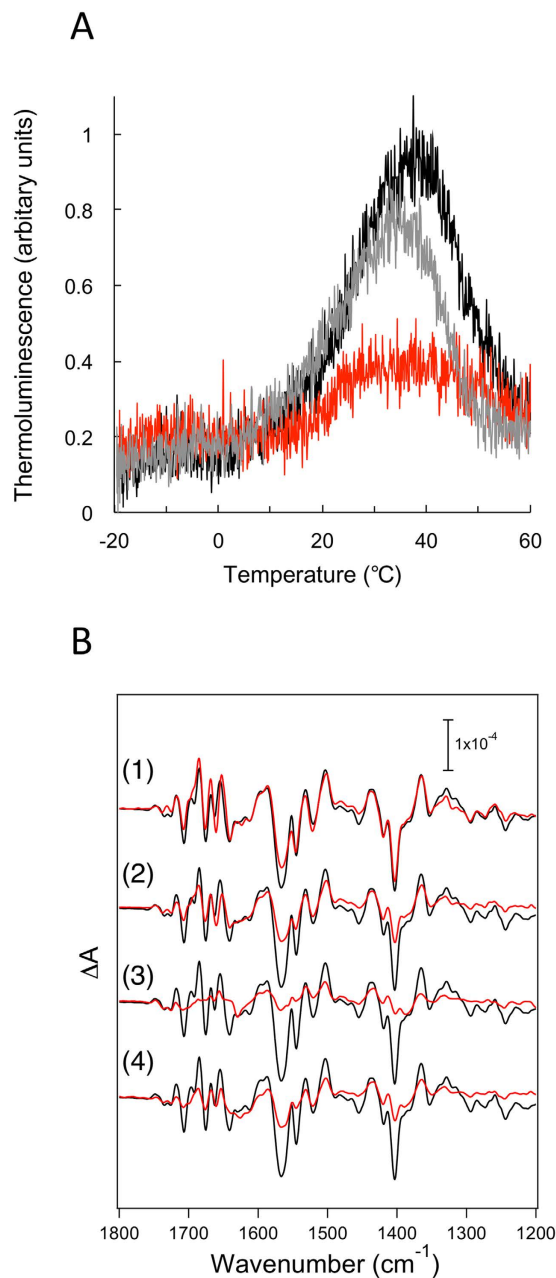


Figure 5. The pN15 peptide inhibits the S_1 to S_2 transition of the OEC in PSII. (A) Thermoluminescence glow curves of the $S_2/S_3Q_B^-$ charge recombination in NaCl-washed (*black line*), pN15-reconstituted (*red line*) and pN15- ΔA^1 -reconstituted (*grey line*) PSII membranes. (B) The S_2/S_1 FTIR difference spectra of NaCl-washed (*black line*) and pN15- or pN15- ΔA^1 -reconstituted (*red line*) PSII membranes. PSII membranes were reconstituted with pN15 at a molar pN15:PSII ratio of 50:1 (1), 100:1 (2), and 200:1 (3) and with pN15- ΔA^1 at 200:1 (4).

amount of PsbP enables photoautotrophic growth and subsequent accumulation of the PSII reaction centre^{21–24}. In higher plants, the *de novo* biogenesis of PSII, as well as the repair of photo-damaged PSII, occurs in stroma-exposed thylakoid membranes, while the PSII supercomplex accumulates in the stacked granal regions⁴⁶. It was observed that the LP form of Cyt *b*₅₅₉ is mostly present in the stromal membranes, while the HP form is enriched in the grana⁴⁷. PsbP mainly localizes to the grana, but a significant amount of PsbP is present in a free form, or loosely associated with the thylakoid membranes^{48,49}. Thus it is likely that PsbP does have a role in fine-tuning internal electron transfer within PSII in order to reduce the lifetime of P680⁺ during the assembly of the OEC, protecting it from excess energy.

In cyanobacteria, a PsbP homolog, CyanoP, is proposed to function as an assembly factor for PSII^{50,51}, but its exact function is still unclear⁵². Due to CyanoP not having an N-terminal extension sequence, it is probable that

other proteins may have such a function, similar to our observations with PsbP, in cyanobacteria. A recent study proposed that Psb30, absent in green plants, interacts with PsbF on the lumenal side of the thylakoid membrane and affects the redox properties of Cyt b_{559} in *Synechococcus elongatus*; this would suggest the interaction on the lumenal side can affect the properties of the haem within Cyt b_{559} , a haem that is positioned on the stromal side⁵³. It is also possible that PsbV, which also has an interaction with PsbE in a manner similar to PsbP in the cyanobacterial crystal structure, may have a role to regulate the internal electron transfer within PSII. Further studies are certainly necessary to elucidate how the different composition and expression of the extrinsic proteins among photo-oxygenic organisms contribute in regulating, and tuning the efficiency of, the internal electron transfer of PSII.

Materials and Methods

Preparation of peptide fragments. Peptide fragments were produced by Japan Bio Services (Saitama, Japan). The C-terminus of each peptide fragment was amidated and purity was confirmed to be 95–97% by High-Performance Liquid Chromatography (HPLC). Each peptide powder was dissolved in a MES buffer (25 mM MES-NaOH, pH 6.5) before use.

Plasmid construction, recombinant protein expression and purification. The recombinant PsbP-WT and $-\Delta 9$ proteins from *Spinacia oleracea* (GenBank Accession number, CAA29055.1) were expressed in the *Escherichia coli* strain BL21(DE3) and purified as described previously^{10,54}. The presence of the desired mutation in the recombinant protein was confirmed using MALDI-TOF mass spectrometry (Autoflex III; Bruker Daltonics, MA).

Reconstitution experiments. Reconstitution of the pN15 peptide fragments and PsbP proteins to NaCl-washed PSII membranes was performed based on a procedure reported previously, with some modification⁵⁵. PSII membranes, isolated from spinach leaves⁵⁶, were treated for 30 min with the buffer containing 1.5 M NaCl on ice to remove PsbP and PsbQ. Then pN15 and PsbP were reconstituted with NaCl-washed PSII using a molecular ratio of 50:1, 100:1, or 200:1 (pN15:PSII) and 4:1 (PsbP:PSII). In the control, MES buffer, without any peptide fragments, was used. After incubation for 1 h on ice, the reconstituted PSII samples were carried forward to determine the state of their redox forms of Cyt b_{559} , oxygen-evolving activity, FTIR analysis and TL measurements. Where indicated, PSII samples were washed once, before the analysis, with buffer (25 mM MES-NaOH, pH 6.5, 5 mM NaCl, 5 mM CaCl_2 , 0.4 M sucrose). The oxygen-evolving activity of each PSII membrane sample was measured in this same buffer using a Clark-type oxygen-electrode (Hansatech, UK) in the presence of 0.4 mM 2,6-dichloro-*p*-benzoquinone (DCBQ) as an electron acceptor.

Determination of the redox forms of Cyt b_{559} . PSII membranes were suspended at a Chl concentration of 75 $\mu\text{g ml}^{-1}$ in buffer (25 mM MES-NaOH, pH 6.5, 5 mM NaCl, 5 mM CaCl_2 , 0.4 M sucrose) and the different redox forms of Cyt b_{559} were determined at a wavelength of 559 nm, from the reduced minus oxidized difference absorption spectra between 520 and 580 nm, recorded as described previously^{34,35,57} using a spectrophotometer equipped with a head-on photomultiplier tube (UV-2600; Shimadzu, Kyoto, Japan). Complete oxidation of Cyt b_{559} was achieved by treatment with 2 mM potassium ferricyanide (midpoint redox potential $E_m \sim 430$ mV) followed by its stepwise reduction. The reduction of the HP form ($E_m \sim 400$ mV), the IP form ($E_m \sim 200$ mV), and the LP form ($E_m \sim 50$ mV) of Cyt b_{559} ^{7,58–60} were performed by adding 4 mM hydroquinone ($E_m \sim 280$ mV), 5 mM sodium ascorbate ($E_m \sim 60$ mV), and 10 mM sodium dithionite ($E_m \sim -660$ mV) in a step-wise manner. The absorption difference at 559 nm, in difference spectra of hydroquinone-reduced minus ferricyanide-oxidized, ascorbate-reduced minus hydroquinone-reduced, and dithionite-reduced minus ascorbate-reduced Cyt b_{559} , enable the content of HP, IP, and LP form of Cyt b_{559} , to be deduced, respectively. Baselines were set by drawing a straight line between absorption differences at 540 and 580 nm.

Cross-linking experiments. Cross-linking was performed as described previously^{27,28}. The NaCl-washed PSII membranes, at a concentration of 0.5 mg Chl ml^{-1} , were cross-linked with pN15 peptide fragments in buffer (25 mM MES-NaOH, pH 6.5, 5 mM NaCl, 5 mM CaCl_2 , 0.4 M sucrose) containing 6.25 mM EDC and 5 mM *N*-hydroxysulfosuccinimide (sulfo-NHS). Samples were incubated for 2 h in darkness and the reaction was terminated by adding ammonium acetate to a final concentration of 0.2 M. The cross-linked PSII membranes were subjected to SDS-PAGE via 18% SDS-polyacrylamide gel, and separated proteins were transferred to polyvinylidene difluoride (PVDF) membranes and immuno-detected with specific antibodies. Rabbit antibodies against PsbE and PsbF were purchased from Agrisera AB, Sweden. Rabbit antibody against PsbO was provided by the late Dr. A. Watanabe of Tokyo University. Rabbit antibody against D1 was prepared by the authors.

Thermoluminescence measurements. Thermoluminescence was recorded with an apparatus manufactured by PSI (Brno, Czech Republic). For measurements, a disc of filter paper 5 mm in diameter, was soaked with a total of 10 μg Chl for each PSII sample being investigated. Each disc was then incubated for 2 min at 25 °C in darkness, cooled to -20 °C, and illuminated with a short actinic flash (30 μs). Light emission during sample warming was recorded from -20 °C to 60 °C, at a heating rate of 1 °C s^{-1} .

FTIR analysis. FTIR measurements were performed following the method reported previously^{20,61} with some modifications. NaCl-washed PSII membranes were suspended (2.5 mg Chl ml^{-1}) in a buffer containing 4 mM MES-NaOH, 40 mM sucrose, 5 mM CaCl_2 , and 5 mM NaCl (pH 6.0). An aliquot of the sample (10 μl) was mixed with 1 μl of 20 mM potassium ferricyanide and a desired volume of 5 mM pN15 (1.4, 2.8, and 5.6 μl for the molar ratio of 50, 100, and 200, respectively, of pN15 to PSII), and lightly dried on a CaF_2 plate (25 \times 25 mm) in an oval shape (6 \times 9 mm) under an N_2 gas flow. The resultant sample film was moderately hydrated by sealing

the cell using another CaF₂ plate and a silicone spacer (0.5 mm in thickness) enclosing 2 µl of 40% (v/v) glycerol solution without touching the sample. The sample temperature was adjusted to 10 °C by circulating cold water in a copper holder. Light-induced S₂-minus-S₁ difference spectra (S₂/S₁ spectra) were recorded using a spectrophotometer (VERTEX 80, Bruker Optics) equipped with an MCT detector (InfraRed D313-L) at 4 cm⁻¹ resolution (20, 61). A Ge filter to cut IR light at >2200 cm⁻¹ (Andover, 4.50ILP-25) was placed in the IR path in front of the sample to improve the signal-to-noise ratios of spectra as well as to block a He-Ne laser beam from the interferometer. Illumination was provided by a Q-switched Nd:YAG laser (INDI-40-10; 532 nm, ~7 ns full width at half-maximum, and ~7 mJ pulse⁻¹ cm⁻² at the sample surface; Spectra-Physics, UK). Single-beam spectra were recorded with 100 scans (~50-s accumulation) before and after single-flash illumination to calculate a difference spectrum, and the measurements were repeated 20 times with an interval of 25 min. In the case of pN15-treated samples, measurements with 20 scans were repeated 100 times with an interval of 5 min. This difference in the durations of scans and dark interval is due to faster relaxation of the S₂ state in the pN15-treated samples (τ ~ 20–30 s) than in the NaCl-washed sample (τ ~ 150 s).

References

- Renger, G. & Renger, T. Photosystem II: The machinery of photosynthetic water splitting. *Photosynth. Res.* **98**, 53–80 (2008).
- Umena, Y., Kawakami, K., Shen, J.-R. & Kamiya, N. Crystal structure of oxygen-evolving photosystem II at a resolution of 1.9 Å. *Nature* **473**, 55–60 (2011).
- Suga, M. *et al.* Native structure of photosystem II at 1.95 Å resolution viewed by femtosecond X-ray pulses. *Nature* **517**, 99–103 (2014).
- Renger, G. Photosynthetic water splitting: Apparatus and mechanism. In *Photosynthesis: Plastid Biology, Energy Conversion and Carbon Assimilation*, eds Eaton-Rye, J. J., Tripathy, B. C. & Sharkey, T. D. (Springer, Dordrecht), pp 359–414 (2012).
- Vinyard, D. J., Ananyev, G. M. & Dismukes, G. C. Photosystem II: The reaction center of oxygenic photosynthesis. *Annu. Rev. Biochem.* **82**, 577–606 (2013).
- Shinopoulos, K. E. & Brudvig, G. W. Cytochrome *b*₅₅₉ and cyclic electron transfer within photosystem II. *Biochim. Biophys. Acta* **1817**, 66–75 (2012).
- Kaminskaya, O., Kurreck, J., Irrgang, K. D., Renger, G. & Shuvalov, V. A. Redox and spectral properties of cytochrome *b*₅₅₉ in different preparations of photosystem II. *Biochemistry* **38**, 16223–16235 (1999).
- Hamilton, M. L., Franco, E., Deák, Z., Schlodder, E., Vass, I. & Nixon, P. J. Investigating the photoprotective role of cytochrome *b*-559 in photosystem II in a mutant with altered ligation of the haem. *Plant Cell Physiol.* **55**, 1276–1285 (2014).
- Bricker, T. M., Roose, J. L., Fagerlund, R. D., Frankel, L. K. & Eaton-Rye, J. J. The extrinsic proteins of Photosystem II. *Biochim. Biophys. Acta* **1817**, 121–142 (2012).
- Ifuku, K., Ishihara, S., Shimamoto, R., Ido, K. & Sato, F. Structure, function, and evolution of the PsbP protein family in higher plants. *Photosynth. Res.* **98**, 427–437 (2008).
- Shen, J. R. & Inoue, Y. Binding and functional properties of two new extrinsic components, cytochrome *c*-550 and a 12-kDa protein, in cyanobacterial photosystem II. *Biochemistry* **32**, 1825–1832 (1993).
- Thornton, L. E. *et al.* Homologs of plant PsbP and PsbQ proteins are necessary for regulation of photosystem II activity in cyanobacterium *Synechocystis* 6803. *Plant Cell* **16**, 2164–2175 (2004).
- Ifuku, K., Ido, K. & Sato, F. Molecular functions of PsbP and PsbQ proteins in the photosystem II supercomplex. *J. Photochem. Photobiol. B.* **104**, 158–164 (2011).
- Ifuku, K., Ishihara, S. & Sato, F. Molecular functions of oxygen-evolving complex family proteins in photosynthetic electron flow. *J. Integr. Plant Biol.* **52**, 723–34 (2010).
- Ifuku, K. The PsbP and PsbQ family proteins in the photosynthetic machinery of chloroplasts. *Plant Physiol. Biochem.* **81**, 108–114 (2014).
- Bricker, T. M., Roose, J. L., Zhang, P. & Frankel, L. K. The PsbP family of proteins. *Photosynth. Res.* **116**, 235–250 (2013).
- Ifuku, K. Localization and functional characterization of the extrinsic subunits of photosystem II: an update. *Biosci. Biotechnol. Biochem.* **7**, 1–9 (2015).
- Ghanotakis, D. F., Topper, J. N., Babcock, G. T. & Yocum, C. F. Water-soluble 17 and 23 kDa polypeptides restore oxygen evolution activity by creating a high-affinity binding site for Ca²⁺ on the oxidizing side of Photosystem II. *FEBS Lett.* **170**, 169–173 (1984).
- Miyao, M. & Murata, N. Partial disintegration and reconstitution of the photosynthetic oxygen evolution system. Binding of 24 kilodalton and 18 kilodalton polypeptides. *Biochim. Biophys. Acta* **725**, 87–93 (1983).
- Tomita, M., Ifuku, K., Sato, F. & Noguchi, T. FTIR evidence that the PsbP extrinsic protein induces protein conformational changes around the oxygen-evolving Mn cluster in photosystem II. *Biochemistry* **48**, 6318–6325 (2009).
- Ifuku, K., Yamamoto, Y., Ono, T., Ishihara, S. & Sato, F. PsbP protein, but not PsbQ protein, is essential for the regulation and stabilization of photosystem II in higher plants. *Plant Physiol.* **139**, 1175–1184 (2005).
- Yi, X., Hargett, S. R., Liu, H., Frankel, L. K. & Bricker, T. M. The PsbP protein is required for photosystem II complex assembly/stability and photoautotrophy in *Arabidopsis thaliana*. *J. Biol. Chem.* **282**, 24833–24841 (2007).
- Ido, K. *et al.* Knockdown of the PsbP protein does not prevent assembly of the dimeric PSII core complex but impairs accumulation of photosystem II supercomplexes in tobacco. *Biochim. Biophys. Acta* **1787**, 873–881 (2009).
- Allahverdiyeva, Y. *et al.* Arabidopsis plants lacking PsbQ and PsbR subunits of the oxygen-evolving complex show altered PSII super-complex organization and short-term adaptive mechanisms. *Plant J.* **75**, 671–684 (2013).
- Yi, X., Hargett, S. R., Frankel, L. K. & Bricker, T. M. The PsbQ protein is required in Arabidopsis for photosystem II assembly/stability and photoautotrophy under low light conditions. *J. Biol. Chem.* **281**, 26260–26267 (2006).
- Kakiuchi, S. *et al.* The PsbQ protein stabilizes the functional binding of the PsbP protein to photosystem II in higher plants. *Biochim. Biophys. Acta* **1817**, 1346–1351 (2012).
- Ido, K. *et al.* The conserved His-144 in the PsbP protein is important for the interaction between the PsbP N-terminus and the Cyt *b*₅₅₉ subunit of photosystem II. *J. Biol. Chem.* **287**, 26377–26387 (2012).
- Ido, K. *et al.* Cross-linking evidence for multiple interactions of the PsbP and PsbQ proteins in a higher plant photosystem II supercomplex. *J. Biol. Chem.* **289**, 20150–20157 (2014).
- Ifuku, K. *et al.* Structure and function of the PsbP protein of photosystem II from higher plants. *Photosynth. Res.* **84**, 251–255 (2005).
- Ifuku, K., Nakatsu, T., Kato, H. & Sato, F. Crystal structure of the PsbP protein of photosystem II from *Nicotiana tabacum*. *EMBO Rep.* **5**, 362–367 (2004).
- Cao, P. *et al.* Crystal Structure Analysis of Extrinsic PsbP Protein of Photosystem II Reveals a Manganese-induced Conformational Change. *Mol. Plant* **8**, 664–666 (2015).
- Mummadiseti, M. P. *et al.* Use of protein cross-linking and radiolytic footprinting to elucidate PsbP and PsbQ interactions within higher plant Photosystem II. *Proc. Natl. Acad. Sci. USA* **111**, 16178–16183 (2014).
- Miyao, M., Fujimura, Y. & Murata, N. Partial degradation of the extrinsic 23-kDa protein of the Photosystem II complex of spinach. *Biochim. Biophys. Acta* **936**, 465–474 (1988).

34. Gadjieva, R., Mamedov, F., Renger, G. & Styling, S. Interconversion of low- and high-potential forms of cytochrome b_{559} in tris-washed photosystem II membranes under aerobic and anaerobic conditions. *Biochemistry* **38**, 10578–10584 (1999).
35. Ghanotakis, D. F., Yocum, C. F. & Babcock, G. T. ESR spectroscopy demonstrates that cytochrome b_{559} remains low potential in Ca^{2+} -reactivated, salt-washed PSII particles. *Photosynth. Res.* **9**, 125–134 (1986).
36. Briantais, J. M., Verrotte, C., Miyao, M., Murata, N. & Picaud, M. Relationship between O_2 evolution capacity and cytochrome b -559 high-potential form in Photosystem II particles. *Biochim. Biophys. Acta* **808**, 348–351 (1985).
37. Widger, W. R., Cramer, W. A., Hermodson, M. & Herrmann, R. G. Evidence for a hetero-oligomeric structure of the chloroplast cytochrome b -559. *FEBS Lett.* **191**, 186–190 (1985).
38. Ghanotakis, D. F., Babcock, G. T. & Yocum, C. F. Calcium reconstitutes high rates of oxygen evolution in polypeptide depleted Photosystem II preparations. *FEBS Lett.* **167**, 127–130 (1984).
39. Miyao, M. & Murata, N. Calcium ion can be substituted for the 24-kDa polypeptide in the photosynthetic oxygen evolution. *FEBS Lett.* **168**, 118–120 (1984).
40. Vass, I. & Inoue, Y. Thermoluminescence in the study of photosystem two. In *Topics in Photosynthesis 11*, eds Barber, J. (Elsevier, Amsterdam), pp 259–294 (1992).
41. Sane, P. V. & Rutherford, A. W. Thermoluminescence from Photosynthetic membranes. In *Light Emission by Plants and Bacteria*, eds Govindjee Ames, J. & Fork, D. C. (Academic, Orlando), pp 329–360 (1986).
42. Noguchi, T. Fourier transform infrared difference and time-resolved infrared detection of the electron and proton transfer dynamics in photosynthetic water oxidation. *Biochim. Biophys. Acta* **1847**, 35–45 (2015).
43. Rashid, A. & Carpentier, R. The 16 and 23 kDa extrinsic polypeptides and the associated Ca^{2+} and Cl^- modify atrazine interaction with the Photosystem II core complex. *Photosynth. Res.* **24**, 221–227 (1990).
44. Roose, J. L., Frankel, L. K. & Bricker, T. M. Documentation of significant electron transport defects on the reducing side of photosystem II upon removal of the PsbP and PsbQ extrinsic proteins. *Biochemistry* **49**, 36–41 (2010).
45. Chiu, Y. F. *et al.* Spectroscopic and functional characterization of cyanobacterium *Synechocystis* PCC 6803 mutants on the cytoplasmic-side of cytochrome b_{559} in photosystem II. *Biochim. Biophys. Acta* **1827**, 507–519 (2013).
46. Baena-González, E. & Aro, E. M. Biogenesis, assembly and turnover of photosystem II units. *Philos. Trans. R. Soc. Lond. B. Biol. Sci.* **357**, 1451–1460 (2002).
47. Cox, R. P. & Andersson, B. Lateral and transverse organization of cytochromes in the chloroplast thylakoid membrane. *Biochem. Biophys. Res. Commun.* **103**, 1336–1342 (1981).
48. Hashimoto, A., Yamamoto, Y. & Theg, S. M. Unassembled subunits of the photosynthetic oxygen-evolving complex present in the thylakoid lumen are long-lived and assembly-competent. *FEBS Lett.* **391**, 29–34 (1996).
49. Hashimoto, A., Ettinger, W. F., Yamamoto, Y. & Theg, S. M. Assembly of newly imported oxygen-evolving complex subunits in isolated chloroplasts: sites of assembly and mechanism of binding. *Plant Cell* **9**, 441–452 (1997).
50. Cormann, K. U., Bartsch, M., Rögner, M. & Nowaczyk, M. M. Localization of the CyanoP binding site on photosystem II by surface plasmon resonance spectroscopy. *Front. Plant Sci.* **5**, 1–10 (2014).
51. Jackson, S. A. & Eaton-Rye, J. J. Characterization of a *Synechocystis* sp. PCC 6803 double mutant lacking the CyanoP and Ycf48 proteins of Photosystem II. *Photosynth. Res.* **124**, 217–229 (2015).
52. Aoi, M., Kashino, Y. & Ifuku, K. Function and association of CyanoP in photosystem II of *Synechocystis* sp. PCC 6803. *Res. Chem. Intermed.* **40**, 3209–3217 (2014).
53. Sugiura, M. *et al.* Psb30 contributes to structurally stabilize the Photosystem II complex in the thermophilic cyanobacterium *Thermosynechococcus elongatus*. *Biochim. Biophys. Acta* **1797**, 1546–1554 (2010).
54. Ifuku, K. & Sato, F. Importance of the N-terminal sequence of the extrinsic 23 kDa polypeptide in Photosystem II in ion retention in oxygen evolution. *Biochim. Biophys. Acta* **1546**, 196–204 (2001).
55. Nishimura, T. *et al.* Identification of the basic amino acid residues on the PsbP protein involved in the electrostatic interaction with photosystem II. *Biochim. Biophys. Acta* **1837**, 1447–1453 (2014).
56. Yamamoto, Y., Leng, J. & Shen, J.-R. Isolation of photosystem II-enriched membranes and the oxygen-evolving complex subunit proteins from higher plants. *Methods Mol. Biol.* **684**, 1–10 (2011).
57. Gadjieva, R., Eckert, H. J. & Renger, G. Photoinhibition as a function of the ambient redox potential in tris-washed PSII membrane fragments. *Photosynth. Res.* **63**, 237–248 (2000).
58. Ortega, J. M., Hervás, M. & Losada, M. Redox and acid-base characterization of cytochrome b -559 in photosystem II particles. *Eur. J. Biochem.* **171**, 449–455 (1988).
59. Roncel, M., Ortega, J. M. & Losada, M. Factors determining the special redox properties of photosynthetic cytochrome b_{559} . *Eur. J. Biochem.* **268**, 4961–4968 (2001).
60. Cramer, W. A. & Whitmarsh, J. Photosynthetic cytochromes. *Annu. Rev. Plant Physiol.* **28**, 133–172 (1977).
61. Nagao, R., Tomo, T. & Noguchi, T. Effects of extrinsic proteins on the protein conformation of the oxygen-evolving center in cyanobacterial photosystem II as revealed by Fourier transform infrared spectroscopy. *Biochemistry* **54**, 2022–2031 (2015).
62. Pettersen, E. F. *et al.* UCSF chimera—a visualization system for exploratory research and analysis. *J. Comput. Chem.* **25**, 1605–1612 (2004).

Acknowledgements

This work was supported in part by JST PRESTO (K.I.), by JSPS KAKENHI (grant no. 26660087 to K.I.; 26840091 to R.N.; 24000018 and 25291033 to T.No.), and MEXT KAKENHI (grant no. 24107003 to T.No.). The JST CREST also contributed to this work (part to J.N.). T.Ni. is supported as a JSPS research fellow (grant no. 15J08254).

Additional Information

Supplementary information accompanies this paper at <http://www.nature.com/srep>

Competing financial interests: The authors declare no competing financial interests.

How to cite this article: Nishimura, T. *et al.* The N-terminal sequence of the extrinsic PsbP protein modulates the redox potential of Cyt b_{559} in photosystem II. *Sci. Rep.* **6**, 21490; doi: 10.1038/srep21490 (2016).



This work is licensed under a Creative Commons Attribution 4.0 International License. The images or other third party material in this article are included in the article's Creative Commons license, unless indicated otherwise in the credit line; if the material is not included under the Creative Commons license, users will need to obtain permission from the license holder to reproduce the material. To view a copy of this license, visit <http://creativecommons.org/licenses/by/4.0/>